THE UNIVERSITY OF SYDNEY

Self-interacting scalar field distributions around Schwarzschild black holes

(https://doi.org/10.1103/PhysRevD.107.044070)

Alejandro Aguilar Nieto

Table of contents

Motivation

- Scalar Field models such as BEC's, axion-like particles, and ultralight scalar fields are some of the most promising candidates to explain the nature of dark matter.
- Are black holes a serious threat to scalar field dark matter models? (No: Barranco, et al, 1108.0931)
- From a cosmological perspective, the role of self-interaction is of great importance in dark matter models helping to solve problems such as the cusp-core problem or by increasing the the effective number of relativistic degrees of freedom so that it matches the estimates of BBN.

Klein-Gordon Equation

Let's consider a test massive complex Scalar Field, with its Lagrangian given by

$$\mathscr{L}_\varphi = -\left(\nabla_\mu\varphi\nabla^\mu\varphi^* + \mu^2|\varphi|^2 + \frac{1}{2}\eta\lambda|\varphi|^4\right), \tag{2.1}$$

where $\mu = m/\hbar$ and for convinience, we consider the parameter $\lambda > 0$. The attractive or repulsive nature of the self-interaction is set by $\eta = -1$ and $\eta = 1$ respectively.

We assume that the scalar field is spherically symmetric and thus can be written as

$$\varphi(t, r) = \frac{u(r)}{r}e^{i\omega t}. \tag{2.2}$$

Klein-Gordon Equation

The background metric for the Schwartzschild spacetime is given by

$$ds^2 = -N(r)dt^2 + N^{-1}(r)dr^2 + r^2 d\Omega^2, \tag{2.3}$$

where

$$N(r) = 1 - \frac{2M}{r}. \tag{2.4}$$

The resulting Klein-Gordon equation in Schwarzschild space-time is given by

$$\left[-N(r)\frac{\partial}{\partial r}\left(N(r)\frac{\partial}{\partial r}\right) + V_{\mathrm{eff}}(r)\right] u(r) = \omega^2 u(r), \tag{2.5}$$

where

$$V_{\mathrm{eff}}(r) = N(r)\left[\frac{2M}{r^3} + \mu^2 + \eta\lambda\left(\frac{u^2}{r^2}\right)\right]. \tag{2.6}$$

Scaling Properties

In order to explore the space of solutions of the Klein Gordon equation, we define a new function $v(r)$ as

$$v(r) = \sqrt{\lambda}\, u(r)\,, \tag{2.7}$$

The function v encodes the self interaction parameter and allow us to explore the solution space of Eq. (2.5) providing an infinite set of solutions for each value of λ. Additionally, using the tortoise coordinate, $r* = r + 2M \ln(r/2M - 1)$, we rewrite the KG equation as

$$\left[-\frac{\partial^2}{\partial r^{*2}} + V_{\rm eff}\right] v(r) = \omega^2 v(r), \tag{2.8}$$

The energy density of the scalar field measured by a static observer $\rho = -T_0{}^0$ provides a useful measure of the distribution of the field in the spacetime, however we will focus on the radial energy density $\rho_e = 4\pi r^2 \rho$ which can be obtained through the expression

$$\lambda \rho_e(r) = \frac{1}{2N(r)} \left(\omega^2 v^2(r) + \left(\frac{\partial v}{\partial r^*} \right)^2 + v^2(r) \left(\frac{2M}{r^3} + \mu^2 + \eta \frac{v^2}{r^2} \right) \right), \tag{2.9}$$

Another quantity of interest is the total mass-energy storaged by the scalar field obtained by the integration of the energy density

$$M_\Phi = 4\pi \int_{2M}^{\infty} \rho r^2 dr \,. \tag{2.10}$$

Asymptotic behavior

On the left asymptotic limit $r^* \to -\infty$, $N(r) \to 0$, so the solution of (2.8) will be given by

$$v(r^*) = Acos(\omega r^* + \delta), \tag{2.11}$$

where the amplitude A and the phase δ are real. On the other hand, taking right asymptotic limit $r^* \to \infty$, the effective potential tends to μ^2, so the solution will be given by

$$v(r^*) \propto e^{i\sqrt{\omega^2 - \mu^2} r^*}, \tag{2.12}$$

which will be valid when it decays exponentially, which is satisfied when $0 < \omega^2 < \mu^2$.

Characterization of the solutions

There is a set of discrete values of ω that allows solutions in which the ingoing modes have a larger amplitude than the outgoing modes. These solutions are thus closer to the physical description of having an event horizon as the left boundary.

We find these solutions through the quantity $v_{\max}$, which is defined as the local maximum attained by the function v in the far horizon region, and compare it with the amplitude near the horizon, A, so that these quasi bound or resonant configurations with discrete values for ω correspond to those of when the ratio $A/v_{\max}$ is a minimum.

Characterization of the solutions

In what follows we work with $M\mu = 0.14$. Values of the boson mass μ motivated by dark matter scalar field models correspond to $\hbar\mu \sim 10^{-24}$ eV, and for a black hole with mass $M \sim 10^{8} M_{\odot}$, the gravitational coupling is of the order of $M\mu \sim 10^{-6}$, which is several orders of magnitude different than the ones explored here, however the behaviour of the solutions is expected to remain the same.

Solutions to the KG Equation

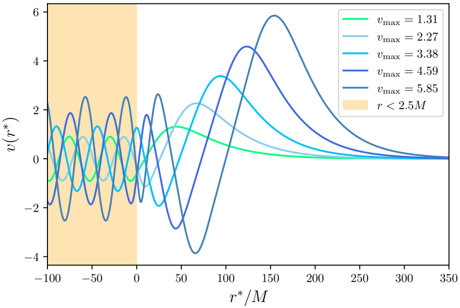

Fig. 3.1: Sample of solutions with an exponential decay at infinity. In the region close the horizon (shaded area, $r* \to -\infty$), the maximal amplitude of the solutions in this region sets the value of A. The value in the far region set by the C also fixes the value of $v_{\text{máx}}$. Thus, each solution can be characterized by the amplitudes A and $v_{\text{máx}}$.

Resonant Frequencies

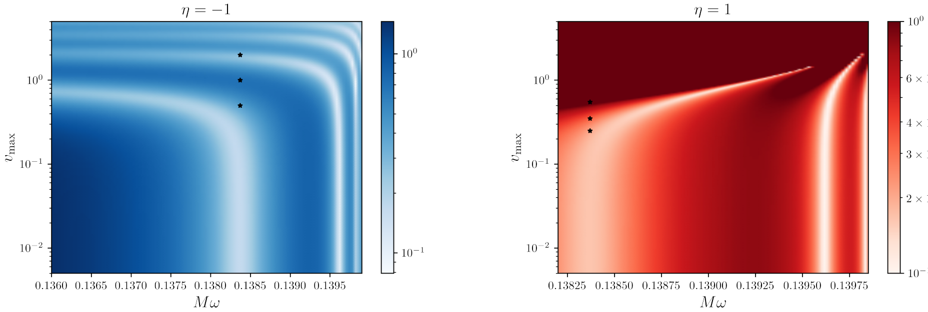

Fig. 3.2: Color map of the ratio $A/v_{\rm max}$ for $M\mu = 0.14$. The intensity of the color indicates the value of the ratio. The white bands, in which the value of $v_{\rm max}$ is much larger than A, correspond to resonant states. Left panel is for $\eta = -1$ and right panel is for $\eta = +1$. The weakly self-interacting regime correspond to the lower part in which $v_{\rm max} \to 0$. For larger values of $v_{\rm max}$ solutions can not be found for $\eta = +1$.

Resonant Frequencies

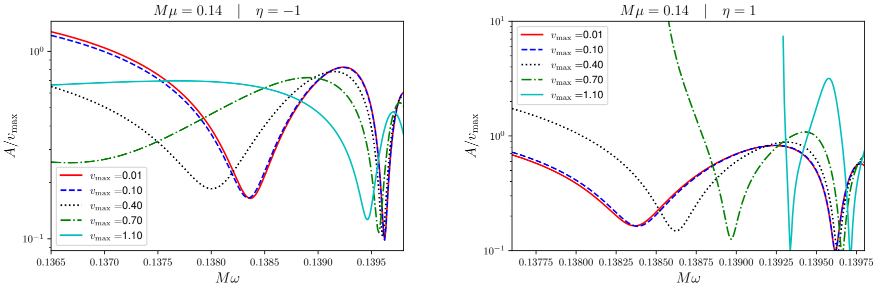

Fig. 3.3: Ratio $A/v_{\rm max}$ as a function of ω for different values of $v_{\rm max}$ and $M\mu = 0.14$. The minimum of each curve denotes a resonant solution.

Resonant States

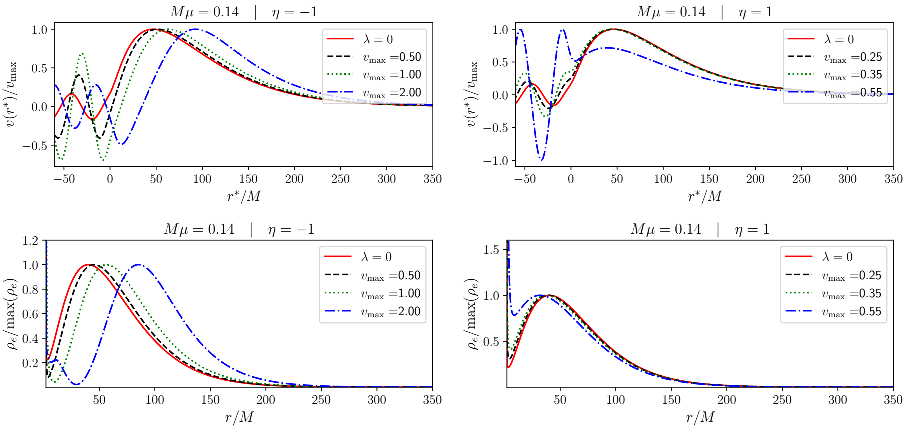

Normalized profile of the scalar field and normalized energy density for a fixed value of $M\omega = 0.13837$ with different values of $v_{\max}$.

Resonant States

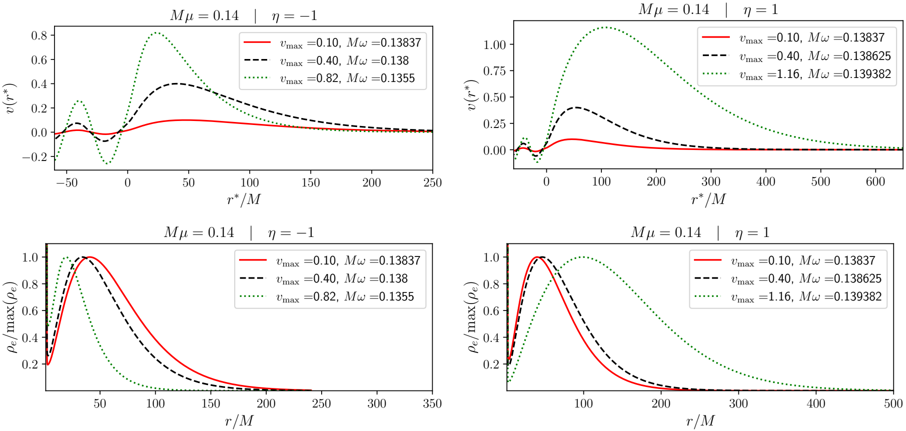

Fig. 3.4: Scalar field profile and Normalized energy density for the first resonant state for different values of $v_{\max}$ for $\eta = -1$, and $\eta = +1$

Resonant States

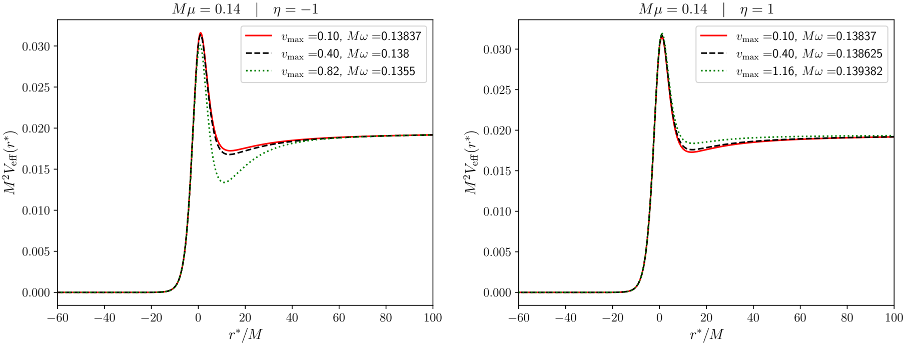

Fig. 3.5: Effective potential for the fundamental states for different values of $v_{\rm max}$. The deep of the potential well increases as $v_{\rm max}$ grows for $\eta = -1$ and decreases for $\eta = +1$. .

Time domain description

Using Eddington-Finkelstein coordinates ($\bar{t}$,r,θ,φ), where $\bar{t} = t + 2Mln(r/2M - 1)$, the Schwarzschild metric can be written as

$$ds^2 = -\left(1 - \frac{2M}{r}\right) d\bar{t}^2 + 4\frac{M}{r} dr d\bar{t} + \left(1 + \frac{2M}{r}\right) dr^2 + r^2 d\Omega^2. \quad (3.1)$$

In terms of Arnowit Desser Misner (ADM) variables, the lapse function α, the shift vector β^r, and the induced 3-metric can be read from Eq. (3.1) as

$$\alpha = \sqrt{\frac{r}{r + 2M}} \qquad \beta^r = \frac{2M}{2M + r} \qquad \gamma_{rr} = 1 + \frac{2M}{r} \,. \quad (3.2)$$

Time domain description

The complex scalar field can be split into 2 real scalar fields according to $\Phi = \varphi_{\mathbf{R}} + i\varphi_{\mathbf{I}}$. The resulting KG equation can be written as a coupled system

$$\nabla_\alpha \nabla^\alpha \varphi_j = \mu^2 \varphi_j + \eta\lambda|\Phi|^2\varphi_j, \tag{3.3}$$

where $|\Phi|^2 = \varphi_R^2 + \varphi_I^2$, and index $j = \mathbf{R}, \mathbf{I}$. In order to solve numerically the Klein-Gordon equation n the background metric (3.1), we introduce the auxiliary first order functions

$$\psi_j = \partial_r \varphi_j \qquad \pi_j = \alpha^2(\partial_t \varphi_j - \beta^r \psi_j) \ . \tag{3.4}$$

Time domain description

Switching to Eddington-Finkelstein and using the ADM variables and the auxiliary first order functions, we find that the 2nd order KG equations is equivalent to the following system of 1st order evolution equations for φ_j, π_j and ψ_j

$$\begin{aligned}
\partial_t\varphi_j &= \frac{r}{r+2M}\left(\pi_j + \frac{2M}{r}\psi_j\right) \,, \\
\partial_t\psi_j &= \frac{2M}{2M+r}\partial_r\psi_j + \frac{r}{2M+r}\partial_r\pi_j + \frac{2M}{(2M+r)^2}\left(\pi_j - \psi_j\right) \,, \\
\partial_t\pi_j &= \frac{1}{2M+r}\left(2M\pi_j + r\psi_j\right) + \frac{2M}{(2M+r)^2}\left(\psi_j - \pi_j\right) \\
&\quad + \frac{2}{r(2M+r)}\left(r\psi_j + 2M\pi_j\right) - \varphi_j\left(\mu^2 + \eta\lambda|\Phi|^2\right) \,. \qquad (3.5)
\end{aligned}$$

Time domain description

The total energy of the Scalar Field configuration in Kerr-Schild coordinates can be written as

$$E = 4\pi \int \rho(r)\alpha r^2 dr \,, \tag{3.6}$$

where

$$\rho(r) = \frac{1}{2}\left(\alpha^2|\pi|^2 + 2\beta^r(\pi_R\psi_R + \pi_I\psi_I) + \gamma^{rr}|\psi|^2 + \mu^2|\Phi|^2 + \frac{1}{2}\lambda|\Phi|^4\right) \,.(3.$$

As a result of the evolution, the scalar field present an oscillating behaviour and a slow rate of decay.

Time domain description

We have used as initial data at $t = 0$ the radial profile of the field $\varphi = \frac{u(r)}{r}$, with $M\mu = 0.12$, $M\mu = 0.14$, $M\mu = 0.16$, and $M\mu = 0.18$ as

$$\begin{aligned} \varphi_R(0,r) &= \varphi(r)\,, \quad \varphi_I(0,r) = 0\,, \\ \pi_R(0,r) &= \alpha^2 \beta^r \partial_r \varphi(r)\,, \quad \pi_I(0,r) = \alpha^2 \omega \varphi(r)\,. \end{aligned} \tag{3.8}$$

We assume that the energy has the form the form $E(t) \sim \exp(-st)$ and perform a linear fit of $\ln(E(t)/E_0)$ with t in order to find the value of the rate of s. The half-lifetime, of the configuration is thus given by $t_{\frac{1}{2}} = \frac{M}{s}\ln(2)$.

Time domain description

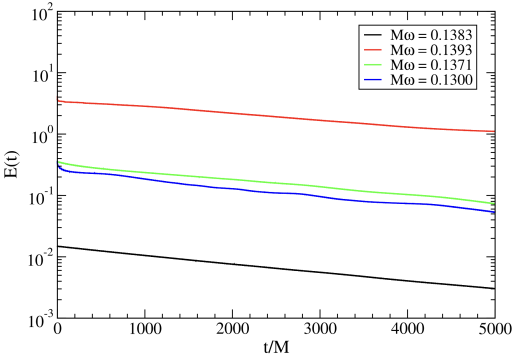

Fig. 3.6: Energy of the scalar field states during the evolution for $M\mu = 0.14$. After an initial fast decay, the energy decays exponentially in time. The rate of decay s, is shown in Table 3.7.

Time Domain description

$M\mu$	$M\omega$	$v_{\max}$	Regime	η	s
0.12	0.1192	0.4548	Weak	+1	$1.16 \pm 0.03 \times 10^{-4}$
0.12	0.1196	1.125	Strong	+1	$8.97 \pm 0.13 \times 10^{-5}$
0.12	0.1180	0.6795	Weak	−1	$1.2 \pm 0.05 \times 10^{-4}$
0.12	0.1100	0.9695	Strong	−1	$1.97 \pm 0.02 \times 10^{-4}$
0.14	0.13837	0.1000	Weak	+1	$3.20 \pm 0.05 \times 10^{-4}$
0.14	0.13930	1.050	Strong	+1	$2.70 \pm 0.07 \times 10^{-4}$
0.14	0.1371	0.6192	Weak	−1	$3.03 \pm 0.07 \times 10^{-4}$
0.14	0.1300	0.9158	Strong	−1	$3.27 \pm 0.07 \times 10^{-4}$
0.16	0.1580	0.4725	Weak	+1	$7.05 \pm 0.05 \times 10^{-4}$
0.16	0.1590	1.102	Strong	+1	$4.41 \pm 0.06 \times 10^{-4}$
0.16	0.1560	0.5564	Weak	−1	$6.93 \pm 0.06 \times 10^{-4}$
0.16	0.1500	0.8580	Strong	−1	$5.45 \pm 0.10 \times 10^{-4}$
0.18	0.1780	0.8232	Weak	+1	$1.41 \pm 0.05 \times 10^{-3}$
0.18	0.1790	1.440	Strong	+1	$5.85 \pm 0.05 \times 10^{-4}$
0.18	0.1750	0.4608	Weak	−1	$1.45 \pm 0.05 \times 10^{-3}$
0.18	0.1700	0.7803	Strong	−1	$9.67 \pm 0.05 \times 10^{-4}$

Fig. 3.7: Parameters of the quasi-resonant states used in the evolution. The last column corresponds to the slope of the line $\ln(E(t)/E_0) = -st$ in Fig. 3.6.

Concluding Remarks

- The values of the discrete resonant frequencies shift as you increase self-interaction. For $\eta = -1$ the frequency decreases and for $\eta = +1$ increases compared with the corresponding values of the frequencies without self-interaction.
- In the regime of strong self-interaction, for $\eta = 1$ the size of the scalar cloud distribution increases considerably and gets away from the horizon as compared to the case with no self-interaction, whereas for $\eta = -1$, the field concentrates closer the horizon with almost no change in size.
- The role of the self-interaction of the scalar field in the life time is negligible as compared to the effect of the mass term. If we use more realistic masses $M\mu \sim 10^{-6}$, then the half-life of the resonant modes can be extrapolated to the order of 10^9 years.

THE UNIVERSITY OF
SYDNEY

Alejandro Aguilar Nieto

Self-interacting scalar field distributions around Schwarzschild black holes

(https://doi.org/10.1103/PhysRevD.107.044070)